Journal of Applied Pharmaceutical Science Vol. 4 (02), pp. 087-100, Feb, 2014
Available online at http://www.japsonline.com
DOI: 10.7324/JAPS.2014.40215
ISSN 2231-3354

CCl_4-induced hepatonephrotoxicity: protective effect of nutraceuticals on inflammatory factors and antioxidative status in rat

Naima Z. Mohamed[1], Howaida I. Abd-Alla[2*], Hanan F. Aly[1], Mona Mantawy[1], Nehal Ibrahim[3], Sohair A. Hassan[1]

[1]Therapeutic Chemistry Department, National Research Centre, Giza, Egypt, [2]Chemistry of Natural Compounds Department, National Research Centre, Giza, Egypt, [3]Pharmacognosy Department, Faculty of Pharmacy, Ain Shams University, Cairo, Egypt.

ARTICLE INFO

Article history:
Received on: 24/07/2013
Revised on: 04/01/2014
Accepted on: 23/02/2014
Available online: 27/02/2014

Key words:
Rumex dentatus, liver fibrosis, renal damage, antioxidants, inflammatory markers, phytoconstituents.

ABSTRACT

The present study was undertaken to investigate the possible protective effect of two edible parts (leaves and stems) of *Rumex dentatus* L. on inflammatory factors and oxidant/antioxidative status of rat. Determination of total phenolic content of the two parts and isolation of bioactive secondary metabolites from the promising leaves extract were carried out. The hepatic antioxidant parameters; glutathione, catalase, superoxide dismutase, glutathione peroxidase, nitric oxide and malondialdehyde were measured. Liver marker enzymes and hepatic function enzymes; aspartate and alanine aminotransferases as well as cholestatic markers; alkaline phosphatase, gamma glutamyltransferase, serum total protein content, urea, creatinine were evaluated. In addition, inflammatory markers; interleukin (IL)-2, IL-6, C-reactive protein, and tumor necrosis factor were estimated. Histopathological investigation was also examined. The ethanolic extract of leaves and stems showed antioxidant properties and anti-inflammatory properties. An improvement of liver and kidney functions was also observed. Extract of leaves showed relatively higher biological activity than that of stems, a fact which may be related to their higher total phenolic content. This extract was subjected to chromatographic and spectroscopic analysis. Phytochemical investigation has afforded emodin (**1**), chrysophanic acid (**2**), 1,5-dihydroxy-3-methyl-9,10-anthraquinone (**3**), quercetin-3-rhamnoside (**4**), quercetin-3-rhamnosyl-(1→6)-galactoside (**5**), Isorhamnetin-3-rhamnoside (**6**), catechin (**7**) and daucosterol (**8**). Compounds **3**-**7** were isolated for the first time from this species. In conclusion, the plant parts extract represents a promising candidate for the treatment of liver fibrosis and renal injury. The isolated bioactive phytochemicals was suggested to be responsible for the pronounced pharmacological activity.

INTRODUCTION

Liver plays a pivotal role in regulating various physiological processes in the body such as metabolism, secretion and storage. It has great capacity to detoxify xenobiotics and synthesize useful principles. Therefore, liver damage inflicted by hepatotoxic agents is of grave consequences (Shanmugasundaram et al., 2006). Evidences developed over the last years have suggested that various forms of liver injuries may be caused by free radical formation and subsequent oxidative stress. Oxidative stress leads to the formation of glycoxidation products, including advanced glycation end products (AGEs) and advanced oxidation protein products (AOPPs). Since advanced oxidation protein products are not only markers of oxidative stress but also act as inflammatory mediators, the knowledge of AOPPs pathophysiology in chronic liver disease could provide valuable information with respect to the relationship between oxidative stress and the inflammatory response related to liver fibrosis (Ali et al., 2011).

Carbon tetrachloride (CCl_4) is one of the xenobiotics that have been reported to induce acute and chronic tissue injuries and is a well established hepatotoxin (Xu et al., 2010). It has been used extensively to study hepatotoxicity in animal models by initiating lipid peroxidation, thereby causing injuries to kidney, heart, testis and brain, in addition to liver pathogenesis (Khan et al., 2012). Liver is particularly susceptible to oxidative stress due to the direct release of CCl_4 metabolites and cytokines, which propagate inflammatory response. CCl_4 was reported to increase serum hepatotoxicity and nephrotoxicity markers. Free radicals play an important role in CCl_4-induced liver and renal damage process (Xu et al., 2010). CCl_4-induced damage is also able to alter the antioxidant status of the tissues, which is manifested by abnormal

* *Corresponding Author*
Howaida Ibrahim Abd-Alla
Tel. number: (+2) 01001455481
E-mail: howaida_nrc@yahoo.com

histopathological changes. Histopathologically, exposure to CCl_4 can result in hepatic steatosis, centrilobular necrosis, and cirrhosis in the liver and acute tubular necrosis in the kidney (Xu et al., 2010; Recknagel et al., 1989).

Alterations in kidney structure and function are frequently encountered in severe liver disease (Lundh, 1964) but the relationship between the hepatic and renal disorders is not clear. The possibilities are that the agent(s) precipitating the liver disease may affect the kidney directly or that the renal lesions develop as a secondary phenomenon to the altered liver function.

In absence of reliable liver protective drugs, therefore, attention is focused on natural antioxidants. Plants offer a wide range of natural antioxidants due to the structural diversities of their secondary metabolites; mainly the phenolic compounds (Xu et al., 2004; Kumar et al., 2012).

Rumex dentatus L (Polygonaceae) is one of eight *Rumex* species native to Egypt (Boulos and El-Hadidi, 1984) and commonly known as toothed dock. Both the leaves and tender stems are traditionally consumed in Egypt and other parts of the world (Tukan et al., 1998). The leaves of a traditional Korean salad plant (*R. acetosa*) were used as food antioxidant (Chon et al., 2008). *Rumex* plants have been used traditionally as a green salad, appetite stimulant, astringent, bactericidal, anti-inflammatory and anti-tumor (Xu et al., 2004). Traditionally *R. crispus* was reported to be used as a botanical hepato-protection during antibiotic therapy (dose of 100-300 mg per day stimulates bile production and release) and a remedy of acute hepatitis, among many traditional folk medicines (Lee et al., 2007).

According to glossary produced by American Diabetics and Association, neutriceutics are substances considered as food or a part of it that offers health or medicinal benefit, including prevention and treatment of diseases (Bloch and Thomson, 1995). Some of the natural products find their use not as pharmaceuticals (real medicine) but as a novel class of dietary supplements or nutraceuticals that fall well into the concept of functional foods.

It is commonly known that *R. dentatus* contains anthraquinones in its roots (Xu et al., 2010). Furthermore, *C*-glucosyl anthrones, naphthalene glucosides, chromones, phytosterols, flavonoids have been detected (Xu et al., 2010; Zhang et al., 2012).

The present study was designed to investigate the protective effect of the two edible parts of *R. dentatus* as neuticeutical agents against the hepatotoxicity and nephrotoxicity induced by CCl_4 which has not previously been explored. The evaluation was done through measuring certain antioxidant parameters, hepatic marker enzymes, liver function indices, cholestatic biomarker and histological investigation of both liver and kidney. The work expanded to investigate the phytochemical constituents from the promising leaves extract.

MATERIAL AND METHODS

General

Mass spectra were recorded on a Finnigan MAT 95 spectrometer (70 eV) (Finnigan MAT, San Jose, CA). UV analyses for pure samples were recorded, separately, in methanol solution and with different diagnostic UV shift reagents on a Shimadzu UV 240 (P/N 240 –58000). The NMR spectra were recorded at 300 and 400 (^{1}H) and 75 and 100 (^{13}C) MHz on Varian Mercury 300 or 400 (Varian, UK) NMR spectrometers; δ values are reported as ppm relative to TMS in the convenient solvent. Gallic acid was purchased from Sigma-Aldrich Chemie (Steinheim, Germany). For column chromatography, Sephadex LH-20 (Pharmacia, Uppsala, Sweden) and silica gel (Si) 60 mesh of 35-60 and 60-120 (E. Merck, Darmstadt, Germany) were used. For paper chromatography (PC), Whatman No. 1 paper sheets (Whatman Ltd., Maidstone, England) and Pre-coated silica gel 60 F_{254} plates for thin layer chromatography (TLC) were used. Solvent systems S_1:C_6H_6-EtOAc (9.5:0.5); S_2:C_6H_{14}-EtOAc (7:3); S_3: $CHCl_3$-MeOH (9.5:0.5); S_4:CH_2Cl_2-CH_3OH (8:2); S_5: CH_2Cl_2-MeOH (8.5:1.5), S_6: *n*-BuOH-HOAc-H_2O (4:1:5, upper layer); S_7: 15 % aqueous HOAc were employed. All chemicals in the present study were of analytical grade, product of Sigma-Aldrich (St. Louis, MO, USA), Merck (Darmstadt, Germany), BDH (Poole, UK) and Riedel de Haën (Seelze, Germany) and were purchased from common sources. The visualization of spots was carried out by spraying with the spray reagents: I. KOH (5% ethanol), II. $AlCl_3$ (1% ethanol), and III. *p*-anisaldehyde-sulphuric acid (AS): 0.5 mL ρ-anisaldehyde is mixed with 10 mL glacial acetic acid, followed by 85 mL methanol and 5 ml concentrated sulfuric acid, and heated to 105°C.

Plant materials

Leaves and stems of *Rumex dentatus* L (Polygonaceae) were collected from Faculty of Agriculture Farm, in March 2010. They were kindly identified by Dr. S.S. El-Khanagry, Department of Flora and Phytotaxonomy Research, Horticultural Research Institute, Egypt. Voucher Specimens were kept in the Herbarium of National Research Centre, Cairo, Egypt. The plant parts were then air-dried in the shade and reduced to powder.

Preparation of samples for biological assays

The dried plant parts (leaves and stems, 1400 g each), were powdered and macerated with 80% aqueous ethanol (3x5 L) for seven days at room temperature. After evaporation of the solvent under reduced pressure, the respective ethanolic extracts were obtained (122 and 98.4 g for leaves and stems, respectively).

Animals

Male Wistar albino rats (100-120 g) were obtained from the Animal House, National Research Centre, Egypt. All animals were kept in controlled environment of air and temperature with access of water and diet. Anesthetic procedures and handling with animals complied with the ethical guidelines of Medical Ethical Committee of National Research Centre in Egypt.

Doses and route of administration

Administration regimen was twice a week for six consecutive weeks. CCl_4 (0.5 mL/kg) was suspended in olive oil (1:9 v/v) and injected intraperitoneally (Marsillach et al., 2009). Leaves and stems extracts were administrated orally at a dose of

200 mg/kg daily for six weeks (Raghavendra and Reddy, 2011). Silymarin; a reference herbal drug was orally administered at a dose of 100 mg/kg, daily for six weeks (Yuvaraj and Subramoniam, 2009). Normal control group received orally 0.5 mL normal physiological saline and intraperitoneally 0.5 mL olive oil. Control groups were treated orally with each extract and with the same dose.

Experimental groups

Seventy male Wistar strain albino rats were used in this study. Animals were divided into 7 groups (10 rats each). Group1 served as normal healthy control rats. Groups 2 and 3 were normal healthy rats administered leaves and stems of *R. dentatus* ethanolic extracts. Group 4 injected with CCl_4. Groups 5 and 6 CCl_4, co–administered with both stem and leaves extract respectively. Group 7 CCl_4 co-administered with silymarin drug.

Sample preparations

Serum sample: Blood collected from each animal by puncture the sublingual vein in clean and dry test tube, left 10 min to clot and centrifuged at 3000 rpm (4°C) for serum separation. The separated serum was stored at -80°C for further determinations of liver and cholestatic function enzymes, kidney markers, inflammatory parameters and serum total protein. Liver tissue was homogenized in normal physiological saline solution (0.9% NaCl) (1:9 w/v). The homogenate was centrifuged at 4°C for 5 min at 3000 rpm. The supernatant was used for estimation of oxidant/antioxidant parameters as well as liver biomarkers of mitochondria; SDH and cell membrane; LDH.

Biochemical assays

Antioxidant parameters

Malondialdehyde, as a product of polyunsaturated fatty acids oxidation was determined (Buege and Aust, 1978) and its concentration was calculated using the extinction coefficient value $1.56 \times 105M^{-1}\ cm^{-1}$ and read at 535 nm. Glutathione was assayed (Moron et al., 1979) using dithiobis-2-nitrobenzoic acid (DTNB) in PBS. The reaction color was read at 412 nm. Superoxide dismutase was estimated (Nishikimi et al., 1972) and the increase in nicotinamide adenine dinucleotide (NADH) oxidation was measured at 560 nm using its molar extinction coefficient $6.22 \times 103\ M^{-1}\ cm^{-1}$. Catalase activity detection was undertaken using a slight modification of the method of Cakmak and Marschner (1992). The reaction mixture, in a total volume of 3 mL, contained 1.5 mL of 50 mM sodium phosphate buffer (pH 7.0) and 1 mL of 0.2% H_2O_2. The reaction was initiated by adding 0.5 mL of the enzyme extract, and the activity determined by measuring the initial rate of disappearance of H_2O_2 at 240 nm. Glutathione peroxidase activity based on a previously reported method (Mohandas et al., 1984) was estimated. There action assay was done in a final volume of 2 mL solution constituted by: 1.49 mL phosphate buffer (0.1 M; pH 7.4), 0.1 mL EDTA (1 mM), 0.1 mL sodium azide (1 mM), 0.05 mL glutathione reductase (1 IU/mL), 0.05 mL GSH (1 mM), 0.1 mL NADPH (0.2 mM), 0.01 mL H_2O_2 (0.25 mM) and 0.1 mL of liver supernatant. The disappearance of NADPH at 340 nm was recorded at 25°C. Enzyme activity was calculated as UM NADPH oxidized/min/mg protein using molar extinction coefficient of $6.22 \times 10^3\ M^{-1}cm^{-1}$. NO-scavenging activity of extracts was determined according to the method of Sreejayan and Rao (1997).

Hepatic cell organelles markers

Succinate dehydrogenase (SDH); a marker for mitochondria was estimated (Rice and Shelton, 1957) and the reduction of flavin adenine dinucleotide was coupled with a reduction of tetrazolium salt as 2-p-iodophenyl-3-p-nitrophenyl-5-phenyl tetrazolium chloride (INT) and the produced formazan of INT was measured colorimetrically at 490 nm. Lactate dehydrogenase (LDH); a marker for cytoplasm was estimated by the method of Babson and Babson (1973), where the reduction of nucleoside derived amino acids (NAD) was coupled with the reduction of tetrazolium salt and the produced formazan of INT was measured colorimetrically at 503 nm.

Serum biomarkers for liver function tests and total protein level

Aspartate and alanine aminotransferases were measured by the method of Gella et al. (1985), where the transfer of amino group from aspartate or alanine formed oxaloacetate or pyruvate, respectively and the developed color was measured at 520 nm. Total protein was assayed (Bradford, 1976) and Coomassie Brilliant Blue dye reacted with Bradford reagent and gave a blue complex at 595 nm. Alkaline phosphatase catalyzed in alkaline medium the transfer of phosphate group from 4 nitrophosphatase to 2-amino-2-methyl-1-propanol (AMP) and librated 4-nitrophenol. The developed colour was measured at 510 nm (Rosalki et al., 1993). Gama glutamyl transferase was estimated (Szasz, 1969), where GGT enzyme reacted with L-g-glutamyl-3-carboxy-*p*-nitroanilide and glycyl-glycine to give L-g-glutamyl-glycyl-glycine and 5-amino-2-nitrobenzoate.The decrease in absorbance was read at 450 nm at 1 min intervals for 3 minutes.

Inflammatory markers

Inflammatory mediators of interleukin (IL)-6, IL-2, tumor necrosis factor (TNF)-α and *C*-reactive protein (CRP) were also estimated using diagnostic kits.

Histopathological investigation

Liver and kidney slices were fixed in 10% formaldehyde and embedded in paraffin wax blocks. Sections of 5 μm thick were stained with hematoxylin and eosin (H&E), then examined under light microscope for determination of pathological changes (Suzuki and Suzuki, 1998).

Determination of total phenolic content

Total phenolic content (TPC) of leaves and stems of *R. dentatus* was, separately, determined spectrophotometrically using the Folin-Ciocalteu reagent (Singleton and Rossi, 1965). Values of TPC were estimated by comparing the absorbance of each sample with a standard response curve generated using gallic acid (0, 12.5, 25, 50, 100, and 200 µg/mL). The results were expressed as mg gallic acid equivalents (GAE)/100 g of each plant part. All the

measurements were taken in triplicate, and the mean values were calculated.

Extraction and isolation of compounds

The fresh leaves (1.4 kg) sample was homogenized in a mixer with aqueous ethanol 80% (3×5 L) followed by exhaustive extraction by maceration at room temperature (48 hrs × 3 times) with the same solvent. The combined extracts were evaporated *in vacuo* at 50 °C to dryness to afford 122.2 g (8.73% wet weight basis). An aliquot of the ethanolic extract (90 g) was subjected to Si column chromatography and the column was eluted in the gradient mode from *n*-hexane gradually to ethyl acetate and then to methanol. Fractions (68, 100 mL each) were collected and monitored by TLC (Si, S_1-S_5). Similar fractions were combined together to obtain 5 groups. These group were further chromatographed on different columns *viz.*, Si column chromatography (eluted successively with a step gradient of *n*-hexane-CH_2Cl_2 (100:0-0:100 v/v) then gradual increase of polarity with methanol) and Sephadex LH-20 (*n*-butanol-*iso*propanol-water, BIW, 4:1:5 (upper phase), methanol or methanol-water mixture (9:1) as different eluents). The homogeneity of the fractions was tested on Comp-TLC (systems S_1-S_5), 2D-PC and Comp-PC using Whatman No. 1 paper (systems S_6 and S_7). Eight major compounds were isolated, their purity being checked by Comp-PC using solvent systems S_1-S_5 for compounds **1**-**3** and **8**, and S_6 and S_7 for compounds **4**-**7** using spray reagent I or III for compounds **1**-**3** and **8**, and II or III for compounds **4**-**7**. These compounds were subjected to physical, chemical, chromatographic and spectral analyses (UV, MS, ^{1}H and ^{13}C NMR) as well as comparison with the available reference standards and available published data.

Compound (**1**): 19 mg, yellow-brown solid, m.p. 254-256 °C, R_f 0.74 (S_3). UV spectral data: λ_{max}, nm (MeOH): 291 and 450. EI-MS: *m/z* (%); 270 (M^+ , 100), 242 ($[M-CO]^+$, 10), 213 (15) , 168 (10), 121 (10). ^{1}H-NMR ($CDCl_3$, 300 MHz): δ ppm 12.30 (1H, s, OH-8), 12.12 (1H, s, OH-1), 11.65 (1H, br s, OH-3), 7.63 (1H, d, *J* =1.2 Hz, H-4), 7.29 (1 H, d, *J* = 2.4 Hz, H-5), 7.10 (1 H, d, *J* =1.2 Hz, H-2), 6.68 (1H, d, *J* =2.4 Hz, H-7), 2.46 (3H, s, CH_3-3), was identified as emodin.

Compound (**2**): 14 mg, orange crystals, m.p. 195-197 °C; R_f 0.61 (S_2), UV λ_{max} nm (MeOH): 217, 276 and 407. EI-MS: *m/z* (%); 254 (M^+, 100), 236 (M^+-H_2O, 75), 226 (80, 225 (12), 208 (7), 198 (10), 197 (20), 180 (4), 169 (12), 152 (14). ^{1}H-NMR ($CDCl_3$, 300 MHz): δ ppm 12.97 (s, OH-1,8), 7.71 (1H, td, *J* = 8.1, 1.2 Hz, H-6), 7.62 (1H, dd, *J* = 8.1, 1.2 Hz, H-5), 7.45 (1H, d, *J* = 1.6, H-4), 7.31 (1H, dd, *J* = 8.2, 1.2 Hz, H-7), 7.03 (1H, d, *J* = 1.6 Hz, H-2), 2.43 (3 H, s, CH_3-3); ^{13}C NMR ($CDCl_3$, 75 MHz): δ ppm 189.4 (C-9), 182.0 (C-10), 162.6 (C-8), 161.6 (C-1), 145.5 (C-3), 136.9 (C-6), 132.7 (C-4a, 5a), 124.7 (C-7), 124.3 (C-2), 118.3 (C-4), 116.2 (C-8a), 112.3 (C-5), 110.0 (C-9a), 23.5 (CH_3-3), was identified as chrysophanic acid.

Compound (**3**): 13 mg, yellow solid, m.p. 227-229 °C; R_f 0.65 (S_2); UV λ_{max} nm (MeOH): 220, 273 and 404. EI-MS: *m/z* (%); 254 (M^+, 100), 226 (15), 225 (8.4), 197 (14.3), 169 (7.5), 141 (10.1). ^{1}H-NMR ($CDCl_3$, 300 MHz): δ ppm 12.13 (s, OH-5), 12.02 (s, OH-1), 7.83 (1H, dd, *J* = 8, 1.2 Hz, H-8), 7.68 (1H, d, *J* = 1.2 Hz, H-4), 7.68 (1H, d, *J* = 8.1 Hz, H-7), 7.31 (1H, dd, *J* = 8.1, 1.2 Hz, H-6), 7.03 (1H, d, *J* =1.2 Hz, H-2), 2.48 (3H, s, CH_3-3); ^{13}C NMR ($CDCl_3$, 75 MHz): δ ppm 192.4 (C-9), 192.3 (C-10), 162.7 (C-5), 162.4 (C-1), 149.3 (C-3), 136.9 (C-7), 133.2 (C-8a), 127.3 (C-4a), 124.5 (C-6), 124.3 (C-4), 121.3 (C-2), 119.9 (C-8), 113.7 (C-5a, 9a), 22.2 (CH_3-3), was identified as 1,5-dihydroxy-3-methyl-9,10-anthraquinone.

Compound (**4**): 18 mg, yellow powder, m.p.180-182 ºC, R_f 0.54 (S_6) and 0.49 (S_7). UV spectral data: λ_{max}, nm (MeOH): 258, 290, 350; (+NaOMe): 270, 325, 390 and 410; (+NaOAc) 268, 375; (NaOAc+H_3BO_3): 260, 370; (+$AlCl_3$) 275, 300, 420; (+$AlCl_3$/HCl): 270, 350, 395. (-) ESI-MS: *m/z* 447 $[M-H]^-$, 483 $[M+Cl]^-$, 895 $[2M-H]^-$. ^{1}H NMR (400 MHz, DMSO-d_6): δ ppm 7.33 (1H, brs, H-2'), 7.29 (1H, brd, *J*=8.4 Hz, H-6'), 6.89 (1H, d, *J*=8.4 Hz, H-5'), 6.41 (1H, brs, H-8), 6.21 (1H, brs, H-6), 5.29 (1H, brs, H-1"), 3.98 (1H, brs, H-2"), 3.53 (1H, dd, *J*=9.5, 3.4 Hz, H-3"), 3.4-3.1 (m, hidden by H_2O-signal, H-4", H-5"), 0.88 (3H, d, *J*=6 Hz, CH_3-6"), APT ^{13}C-NMR (100 MHz, DMSO-d_6): δ ppm 178.3 (C-4), 164.5 (C-7), 161.4 (C-5), 157.5 (C-2), 156.5 (C-9), 148.7 (C-4'), 145.8 (C-3'), 134.9 (C-3), 121.4 (C-6'), 121.3 (C-1'), 116.1 (C-5'), 115.6 (C-2'), 104.3 (C-10), 102.2 (C-1"), 99.3 (C-6), 94.2 (C-8), 71.9 (C-4"), 70.8 (C-3"), 70.9 (C-2"), 70.3 (C-5"), 18.0 (C-6") was identified as quercetin-3-rhamnoside.

Compound (**5**): 12 mg, yellow amorphous, R_f 0.50 (S_6), 0.43 (S_7). UV: λ_{max} nm (MeOH): 250 sh, 269, 340; (+NaOMe): 273, 296 sh, 376; (+$AlCl_3$): 272, 303 sh, 427; (+$AlCl_3$+HCl): 272, 303 sh, 351; (+NaOAc): 266, 299 sh, 400; (+ NaOAc + H_3BO_3): 266, 399 sh, 400 nm. CI-MS *m/z* (100 %): 611 ($[M+H]^+$, 23), 465 ($[M-deoxyrhamnose+2H]^+$, 14.5), 303 ($[M-deoxyrobinose+2H]^+$, 100). ^{1}H NMR (DMSO-d_6, 300 MHz): δ ppm 7.30 (2 H, m, H-2'/6') ; 6.53 (1 H, d, *J*= 8.4 Hz, H-5'), 6.02 (1H, d, *J*= 1.8 Hz, H-8), 5.88 (1 H, d, *J*= 1.8 Hz, H-6), 4.60 (1 H, d, *J*=7.5 Hz, H-1"), 4.24 (1 H, brs, H-1"), 3.80- 3.04 (m, sugar protons), 0.77 (3 H, d, *J*= 6 Hz, CH_3-6'"), ^{13}C NMR (DMSO-d_6,75 MHz): δ ppm 177.9 (C-4), 164.4 (C-7), 161.4 (C-5), 157.5 (C-9), 156.6 (C-2), 148.1 (C-4'), 144.2 (C-3'), 134.3 (C-3), 122.1 (C-6'), 121.3 (C-1'), 116.6 (C-5'), 115.4 (C-2'), 100.8 (C-1'"), 104.3 (C-10), 99.4 (C-6/1"), 93.9 (C-8), 75.3 (C-5"), 74.0 (C-3"), 72.8 (C-4'"), 70.9 (C-2'"), 70.3 (C-2"/3'"), 69.6 (C-4"/5'"), 69.7 (C-4"), 67.0 (C-6"), 17.3 (C-6'"),was identified as quercetin-3-rhamnosyl-(1→6)-galactoside.

Compound (**6**): 15 mg, yellow powder, m.p. 176-178°C, R_f 0.58 (S_6), 0.44 (S_7). EI–MS: *m/z* 316 $[aglycone+H]^+$, +ve ESI–MS: *m/z* 462 $[M+H^+]$. UV spectral data: λ_{max}, nm (MeOH): 256, 330; (+NaOMe): 261, 328, 392; (+NaOAc): 266, 339; (NaOAc+H_3BO_3): 260, 268; (+$AlCl_3$): 271, 328, 397; (+$AlCl_3$/HCl): 269, 363, 396. ^{1}H NMR (DMSO-d_6, 300 MHz): δ ppm 12.52 (1H, s, OH-5), 7.32 (1H, d, *J*=2.0 Hz, H-2'), 7.21 (1H, d, *J*= 8.0 Hz, H-6'), 6.80 (1H, d, *J*=8.0 Hz, H-5'), 6.31 (1H, d, *J*=2.2 Hz, H-8), 6.10 (1H, d, *J*=2Hz, H-6), 5.21 (1H, d, *J*=1.2 Hz, H-1"), 3.99 (s, OCH_3), 3.1-3.9 (m, two sugar protons), and 0.90 (3 H, d, *J*=6.0 Hz, CH_3-rhamnosyl). ^{13}C NMR (DMSO-d_6, 75 MHz): δ ppm 177.4 (C-4), 165.7 (C-7), 161.2 (C-2), 156.9 (C-5), 156.5 (C-9), 148.6 (C-4'), 147.2 (C-3'), 134.1 (C-3), 121.0 (C-6'), 103.4 (C-10), 99.0 (C-6), 93.8 (C-8), 120.6 (C-1'), 115.5 (C-5'), 115.4 (C-2'), 101.8 (C-1"), 71.2 (C-4"), 70.5 (C-2"), 70.4 (C-3"), 70.0 (C-5"),

56.0 (OCH_3), 17.4 (CH_3-rhamnose), was identified as Isorhamnetin-3-rhamnoside.

Compound (**7**): 18 mg, yellowish brown powder, m.p. 148-150 °C, R_f 0.49 (S_3). UV spectral data: λ_{max}, nm (MeOH): 227, 277. ^{1}H NMR (DMSO- d_6, 300 MHz): δ ppm 6.74 (1H, d, *J*=2.1 Hz, H-2'), 6.69 (1H, d, *J*=8.1 Hz, H-5'), 6.60 (1H, dd, *J*= 1.8, 6.5 Hz, H-6'), 5.89 (1H, d, *J*=2.4 Hz, H-8), 5.70 (1H, d, *J*=2.1 Hz, H-6), 4.49 (1H, d, *J*=7.2 Hz, H-2), 3.83 (1H, d, *J*=6.9 Hz, H-3), 2.68 (1H, dd, *J*=5.4, 10.8 Hz, H-4), 2.37 (1H, dd, *J*= 8.1, 7.8 Hz, H-5), was identified as catechin.

Compound (**8**): 22 mg, white powder, 280-281°C; R_f 0.53 (S_5). (-) ESI-MS/MS *m/z* (100 %): 1150 [2 M-H]$^-$, 575 [M-H]$^-$; ^{1}H NMR (DMSO-d_6, 300 MHz): δ ppm 5.32 (1H, brs, H-6), 4.20 (1H, d, *J*=7.8 Hz, H-1'), 3.61 (1H, m, H-3), 3.40-2.90 (1H, d, H-2'); ^{13}C NMR (DMSO-d_6, 75 MHz): δ ppm 140.4 (C-5), 121.1 (C-6), 100.8 (C-1'), 77.0 (C-3'/5'), 76.7 (C-3), 73.4 (C-2'), 70.0 (C-4'), 61.0 (C-6'), 56.2 (C-14), 55.0 (C-17), 45.1 (C-24), 49.6 (C-9), 45.1 (C-24), 41.8 (C-13), 39.7 (C-12), 38.3 (C-4), 36.8 (C-1), 36.2 (C-10), 35.8 (C-20), 33.8 (C-22), 31.4 (C-7/8), 29.5 (C-25), 29.2 (C-2), 28.7 (C-16), 26.1 (C-23), 24.8 (C-15), 22.6 (C-28), 20.9 (C-11), 19.6 (C-26), 18.9 (C-27), 18.6 (C-21), 19.0 (C-19), 11.7 (C-29), 11.6 (C-18), was identified as 3-*O*-β-D-glucopyranosyl-β-sitosterol (daucosterol).

Statistical analysis and calculations

All data were expressed as mean ± SD of ten rats in each group. Statistical analysis was carried out by one way analysis of variance (ANOVA) and Costat Software Computer Program. Significance difference between groups was at $p \leq 0.05$.

% change = (control mean - treated mean)/control mean × 100.

% improvement = treated mean - injured mean/control mean × 100.

RESULTS

Extracts safety

Normal healthy rats administrated with leaves and stems ethanol extract recorded insignificant changes in all parameters under investigation revealing extracts safety.

Effect of *R. dentatus* leaves and stems extract on hepatic antioxidant levels

CCl_4 group recorded significant decrease in GSH (65.59%), GPX (58.14%) and SOD (47.14%) levels, while MDA showed significant increase by 92.20%. Total protein content showed significant decrease in CCl_4 intoxicated rats by percentage decrease reached to 30.34% (Table 1). Treatment with leaves and stems ethanol extract improved MDA level by 10.39, 9.09%, GPX by 42.63, 46.51%, and SOD levels by 30.59 and 23.01%, respectively. GSH levels have been enhanced after treatment with leaves and stems extract by 28.66 and 32.41%, respectively. Also, ethanol extract of *R. dentatus* leaves and stems improved serum total protein by 38.32 and 34.21%, respectively. Similar results were noticed for treatment with silymarin showed ameliorated percent reached to 40.52, 34.11, 4.51, 3.84, 35.73%, GSH, GPX, MDA, SOD and total protein content respectively.

Effect of *R. dentatus* leaves and stems extract on hepatic marker enzymes

Fibrotic liver induced by CCl_4 showed significant decrease in SDH, LDH by 12.42, 32.12% respectively (Table 2). Treatment with *R. dentatus* extracts displayed improvement in marker enzymes. Ethanolic leaves and stems extract showed similar improvement percentages (13.85 and 32.33% for SDH and LDH respectively). However treatment with silymarin improved SDH and LDH by 12.13 and 28.88%, respectively.

Potency of *Rumex dentatus* in improving liver function enzymes

CCl_4 group, showed significant increase in AST and ALT levels by 148.41 and 66.79%, respectively (Table 3). However, GGT and ALP were significantly increased by 77.79 and 97.40%, respectively in CCl_4 group. The observed changes in liver function enzymes showed that leaves and stems extract recorded the same improvement percentages. AST and ALT were ameliorated by 90.30 and 40.35%, while ALP was improved by 70.34 and 81.28%, for the two extracts, respectively. GGT recoded enhanced level of 77.98 and –60.64%, respectively. On the other hand, silymarin exhibited ameliorating percent of 93.90, 41.98, 68.03 and 71.39%, for AST, ALT, GGT and ALP levels, respectively.

Effect of ethanol extract of *Rumex dentatus* on kidney-function

As compared to normal healthy rats, CCl_4 group recorded significant increase in urea and creatinine levels by 127.07 and 40.00%, respectively (Table 4). Improvement in urea and creatinine after treatment revealed that leaves and stems extract showed an improvement by high percentages. Treatment with ethanol leaves and stems extract recorded improvment percent in urea reaching 132.92, and 157.07% and for creatinine 47.00 and 44.00 %, respectively. While, urea and creatinine recorded improvement percentages reaching 159.57 and 44.00 % post silymarin treatment.

Efficiency of *Rumex dentatus* on inflammatory markers

Liver injury induced by CCl_4 showed significant increase in inflammatory markers IL-2, IL-6, TNF-α and CRP by 54.32, 212.91, 169.56 and 108.72% respectively (Table 5). Treatment with *R. dentatus* extracts displayed improvement in inflammatory markers; with ethanolic leaves extract showing higher improvement percentages than stems one. It showed 49.71, 166.67, 159.42 and 90.31% for IL-2, IL-6, TNF-α and CRP, respectively. Treatment with silymarin improved IL-2, IL-6, TNF-α and CRP by 51.88, 167.01, 156.52 and 77.54%, respectively.

Hepato-renal histopathological investigations

Liver of CCl_4-intoxicated rat showed Kupffer cells activation, necrosis of sporadic hepatocytes, fatty degeneration of

Table 1. Effect of *R. dentatus* leaves and stems extract on hepatic oxidant/antioxidant (GSH, MDA, NO, GPX, CAT and SOD) levels and total hepatic protein content in CCl_4 intoxicated rats.

Groups / Parameters	Normal Control	Normal control treated with leaves extract	Normal control treated with stems	CCl_4 group	CCl_4 treated with leaves extract	CCl_4 treated with stems extract	CCl_4 treated with silymarin
Glutathione (GSH)	799.65±69.3$^{(a)}$	739.88±34.0$^{(a)}$	744.19±32.0$^{(a)}$	275.10.±49.2$^{(d)}$	504.26±59.49$^{(c)}$	534.26±44.9$^{(c)}$	599.16±128.39$^{(b)}$
Malondialdehyde (MDA)	0.77±0.11$^{(b)}$	0.78±0.07$^{(b)}$	0.76±0.04$^{(b)}$	1.48±0.25$^{(a)}$	0. 79±0.04$^{(b)}$	0. 78±0.02$^{(b)}$	0.73±0.03$^{(b)}$
Nitric oxide (NO)	12.93±2.54$^{(c)}$	12.03±2.94$^{(c)}$	11.99±1.64$^{(c)}$	54.50±7.12$^{(f)}$	14.40±2.10$^{(c)}$	15.50±1.92$^{(c)}$	19.54±2.12$^{(c)}$
Glutathione peroxidase (GPX)	1.29±0.016$^{(a)}$	1.26±0.012$^{(a)}$	1.32±0.05$^{(a)}$	0.54±0.03$^{(b)}$	1.09±0.01$^{(a)}$	1.14 ±0.02$^{(a)}$	0.98 ±0.04$^{(a)}$
Catalase (CAT)	11.40±1.19$^{(b)}$	11.49±1.10$^{(b)}$	11.68±1.37$^{(b)}$	12.99±0.18$^{(c)}$	11.70±0.68$^{(b)}$	11.00 ±0.55$^{(b)}$	11.65 ±0.18$^{(b)}$
Superoxide dismutase (SOD)	15.95±2.69$^{(a)}$	16.05±2.00$^{(a)}$	16.78±1.10$^{(a)}$	8.430±0.96$^{(b)}$	13.31±2.53$^{(b)}$	12.10±2.23$^{(b)}$	9.15±2.70$^{(b)}$
Total hepatic protein (HP)	129.2±6.35$^{(c)}$	133.0±4.99$^{(c)}$	130.10±7.06$^{(c)}$	90.00±6.00$^{(a)}$	139.50±8.14$^{(c)}$	134.2±7.00$^{(c)}$	136.16±6.49$^{(c)}$

Data presented as means ± SD of ten rats in each group. Data are expressed as µg/mg protein for glutathione, µmoL/mg protein for lipid peroxides and superoxide dismutase, mg/ml for total protein content. Unshared letters between groups are the significance values at P≤ 0.05.

Table 2. Effect of *R. dentatus* leaves and stems extract on liver function markers SDH and LDH following CCl_4 intoxication in rats.

Groups / Parameters	Normal control	Normal control treated with leaves extract	Normal control treated with stems extract	CCl_4 group	CCl_4 treated with leaves extract	CCl_4 treated with stems extract	CCl_4 treated with silymarin
Succinate dehydrogenase (SDH)	100.80±25.8$^{(a)}$	106.19±15.93$^{(a)}$	103.39±12.51$^{(a)}$	88.28 ±20.21$^{(b)}$	99.28±10.05$^{(a)}$	97.00±7.00$^{(a)}$	101.16±6.19$^{(a)}$
Lactate dehydrogenase (LDH)	135.88±19.18$^{(a)}$	139.19±8.46$^{(a)}$	138.16±9.45$^{(a)}$	92.11±32.109$^{(b)}$	124.90±12.63$^{(a)}$	136.04±17.00$^{(a)}$	131.2±35.16$^{(a)}$

Data presented as means ± SD of ten rats in each group.. Data are expressed as Unit/mg protein. Unshared letters between groups are the significance values at P≤0.05.

Table 3. Effect of *R. dentatus* leaves and stems extract on liver function enzymes; AST, ALT, ALP and GGT in CCl_4 treated rats.

Groups / Parameters	Normal control	Normal control treated with leaves extract	Normal control treated with stems extract	CCl_4 group	CCl_4 treated with leaf extract	CCl_4 treated with stems extract	CCl_4 treated with silymarin
Aspartate aminotransferase (AST)	16.09±1.60$^{(c)}$	17.39±1.07$^{(c)}$	18.22±1.43$^{(c)}$	39.97±4.00$^{(a)}$	25.44±2.00$^{(c)}$	23.04±4.50$^{(c)}$	24.86±3.37$^{(c)}$
Alanine aminotransferase (ALT)	32.56±2.02$^{(b)}$	30.50±4.02$^{(b)}$	32.64±9.31$^{(b)}$	54.31±5.29$^{(a)}$	41.17±8.38$^{(ab)}$	39.90±8.38$^{(ab)}$	40.64±7.72$^{(ab)}$
Gamma glutamyl transferase (GGT)	16.08±1.50$^{(c)}$	16.78±1.63$^{(c)}$	17.68±5.93$^{(c)}$	28.59±4.48$^{(b)}$	16.05±2.49$^{(c)}$	17.23±3.21$^{(b)}$	17.65±5.46$^{(c)}$
Alkaline phosphatase (ALP)	12.34±2.41$^{(b)}$	13.86±0.48$^{(b)}$	13.57±2.49$^{(b)}$	24.36±2.97$^{(a)}$	15.68±5.82$^{(b)}$	14.33±4.12$^{(b)}$	15.55±3.00$^{(b)}$

Data presented as means ± SD of ten rats in each group.. Data are expressed as Unit/mg protein. Unshared letters between groups are the significance values at P≤0.05.

Table 4. Effect of *R. dentatus* leaves and stems extract on kidney-function tests in CCl_4 intoxicated rats

Groups / Parameters	Negative controls			CCl_4 group	Treated rats		
	Normal Control	Normal control Treated leaves extract	Normal control Treated stems extract		CCl_4 Treated leaves extract	CCl_4 Treated stems Extract	Silymarin
Urea (mg/dL)	40.00±0.51$^{(a)}$	30.00±0.57$^{(a)}$	27.00±0.57$^{(a)}$	90.83±4.63$^{(b)}$	37.66±1.45$^{(a)}$	28.00±0.57$^{(a)}$	27.00±1.37$^{(a)}$
Creatinine(mg/dL)	1.00±0.05$^{(a)}$	0.93±0.03$^{(a)}$	1.00±0.05$^{(a)}$	1.4 ±0.11$^{(b)}$	0.93± 0.08$^{(a)}$	0.96±0.03$^{(a)}$	0.96±0.03$^{(a)}$

Data presented as means ± SD of ten rats in each group.. Data are expressed as Unit/mg protein. Unshared letters between groups are the significance values at P≤0.05.

Table 5. Effect of *R. dentatus* leaves and stems extract on inflammatory markers in CCl_4 intoxicated rats.

Groups / Parameters	Normal control	Normal control treated with leaves	Normal control treated with stems	CCl_4 group	CCl_4 treated with leaves extract	CCl_4 treated with stems extract	CCl_4 treated with silymarin
Interleukin-2 (IL-2)	129.12±15.60$^{(a)}$	126.02±9.68$^{(a)}$	126.02±7.98$^{(a)}$	199.27±33.01$^{(b)}$	142.28±22.20$^{(a)}$	135.08±19.11$^{(a)}$	132.28±21.00$^{(a)}$
Interleukin-6 (IL-6)	28.80±3.68$^{(a)}$	25.88±2.08$^{(a)}$	25.00±3.18$^{(a)}$	90.12±9.60$^{(b)}$	45.92±4.98$^{(a)}$	42.12±8.60$^{(a)}$	42.02±7.68$^{(a)}$
Tumor necrosis factor (TNF-α)	0.69±0.001$^{(a)}$	0.60±0.002$^{(a)}$	0.63±0.004$^{(a)}$	1.86±0.46$^{(b)}$	0.82±0.46$^{(a)}$	0.76±0.46$^{(a)}$	0.78±0.46$^{(a)}$
C-reactive protein (CRP)	6.19±0.20$^{(c)}$	5.82±0.14$^{(c)}$	6.12±0.50$^{(c)}$	12.92±0.99$^{(d)}$	7.92±0.89$^{(c)}$	7.33±0.74$^{(c)}$	8.12±0.99$^{(c)}$

All inflammatory markers are expressed as (ηg/mL). Data are means ± SD of ten rats in each group. Unshared letters between groups are the significance values at P≤0.05.

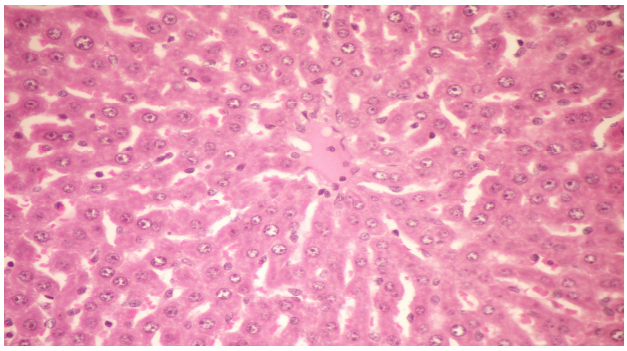

Fig. 1: Liver of normal control rat showing no histopathological changes (H & E X 400).

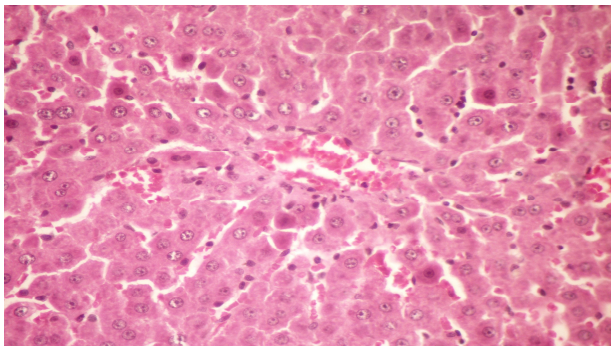

Fig. 2: Liver of CCl_4 intoxicated rat showing congestion of central vein, Kupffer cells activation and necrosis of sporadic hepatocytes (H & E X 400).

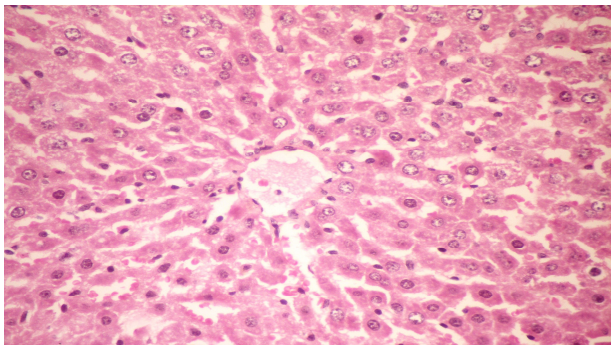

Fig. 3: Liver of CCl_4 intoxicated rat showing Kupffer cells activation and necrosis of sporadic hepatocytes (H & E X 400).

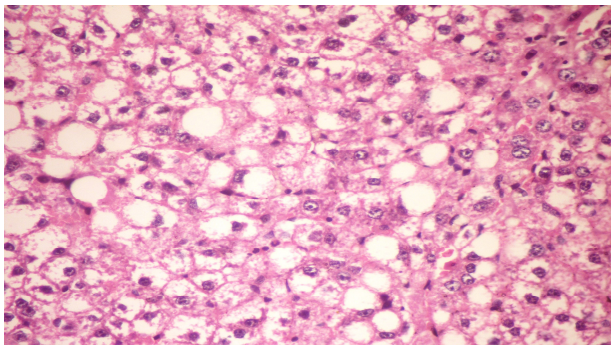

Fig. 4: Liver of CCl_4 intoxicated rat showing fatty degeneration of hepatocytes (H & E X 400).

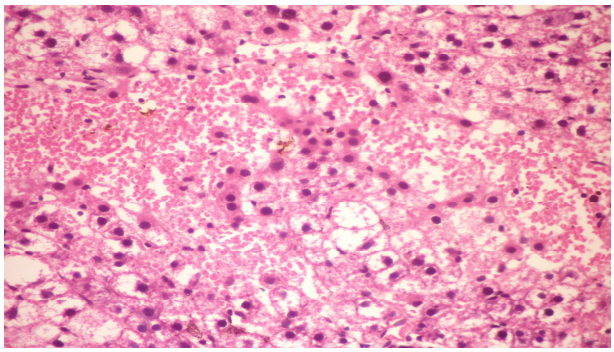

Fig. 5: Liver of CCl_4 intoxicated rat showing fatty degeneration of hepatocytes, pyknosis of hepatocytic nuclei and focal hepatic hemorrhage. (H & E X 400).

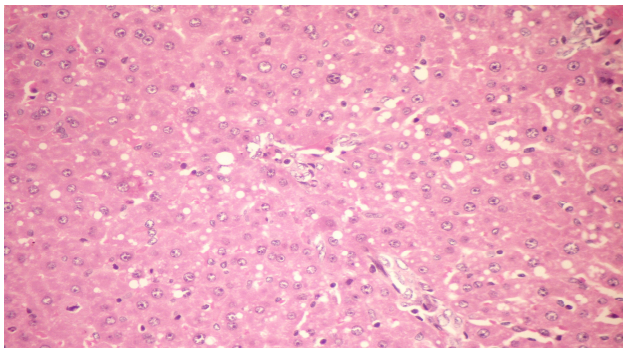

Fig. 6: Liver of CCl_4 intoxicated rat treated with leaf total extract of Rumex dentatus showing few fatty degeneration of hepatocytes and Kupffer cells activation (H & E X 400).

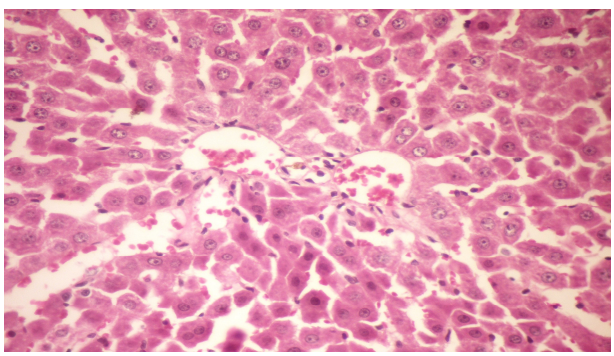

Fig. 7: Liver of CCl_4 intoxicated rat treated with stem total extract of Rumex dentatus showing slightly Kupffer cells activation and few necrosis of sporadic hepatocytes H & E X 400).

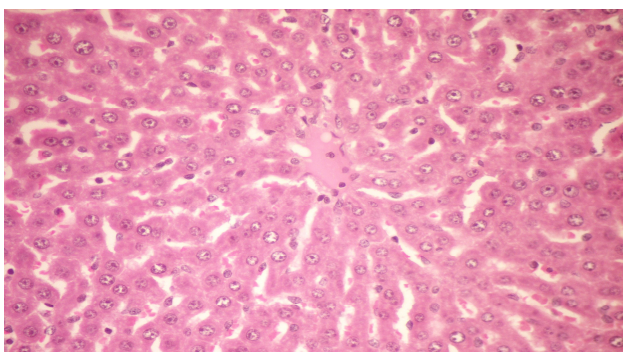

Fig. 8: Liver of CCl_4 intoxicated rat treated with silymarin showing slight dilatation of hepatic sinusoids associated with Kuffer cells activation (H & E X 400).

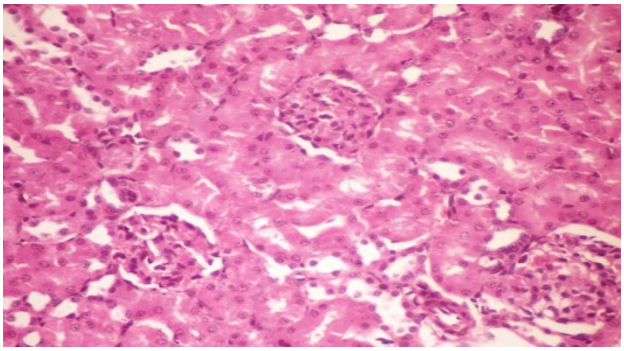

Fig. 9: Kidney of normal control rat showing no histopathological changes. (H & E X 400).

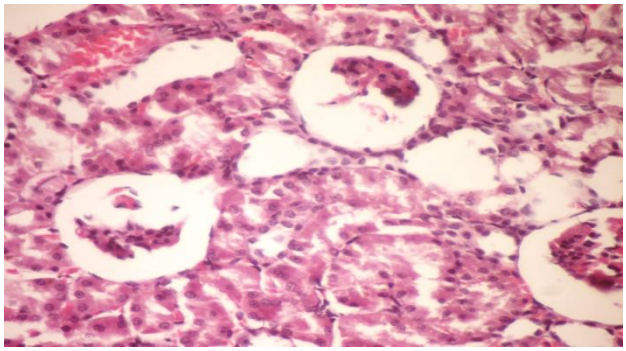

Fig. 10: Kidney of CCl_4 Intoxicated rat showing congestion of glomerular tufts and vacuolization of epithelial lining renal tubules (H & E X 400).

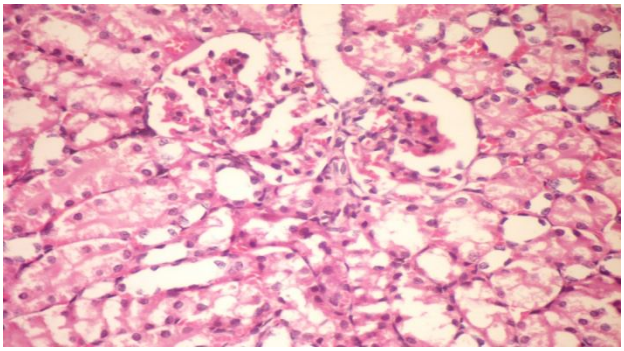

Fig. 11: Kidney of CCl_4 intoxicated rat showing atrophy of glomerular tufts and distension of Bowman's space (H & E X 400).

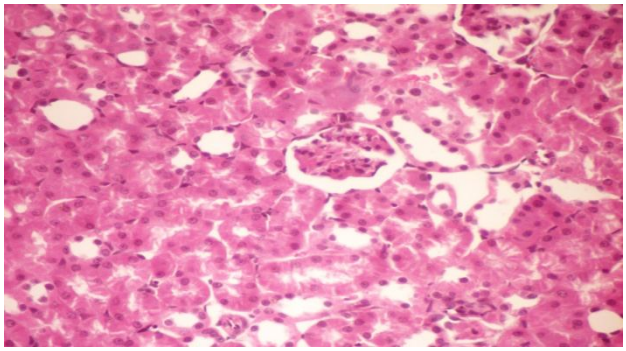

Fig. 12: Kidney of CCl_4 intoxicated rat showing atrophy of glomerular tufts and apparent normal renal parenchyma (H & E X 400).

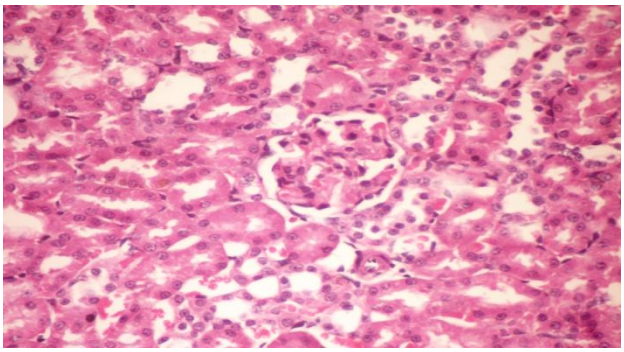

Fig. 13: Kidney of rat CCl_4 intoxicated rat treated with leaf total extract of *Rumex dentatus* showing no histopathological changes (H & E X 400).

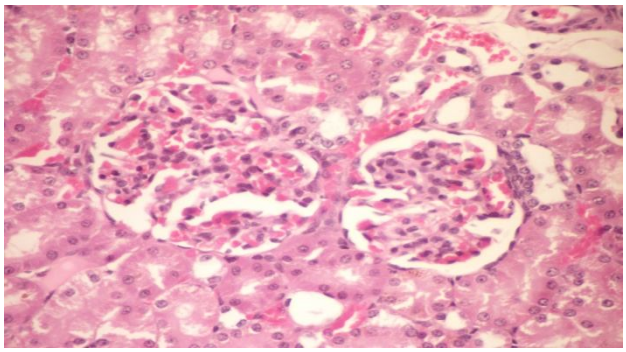

Fig. 14: Kidney of CCl_4 intoxicated rat treated with stem total extract of *Rumex dentatus* showing slight congestion of glomerular tufts and slight congestion of intertubular blood capillaries. (H & E X 400).

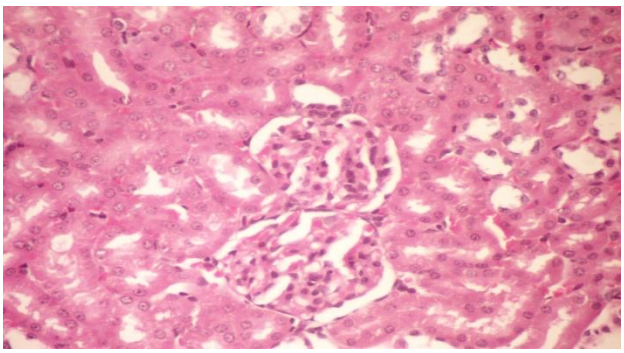

Fig. 15: Kidney of CCl_4 intoxicated rat treated with stem total extract of *Rumex dentatus* showing apparent normal renal parenchyma. (H & E X 400).

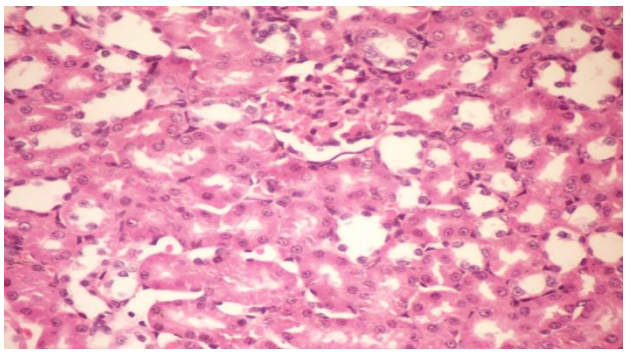

Fig. 16: Kidney of CCl_4 intoxicated rat treated with silymarin showing no histopathological changes (H & E X 400).

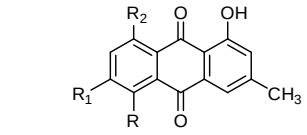

Compound	R	R_1	R_2
1	H	OH	OH
2	H	H	OH
3	OH	H	H

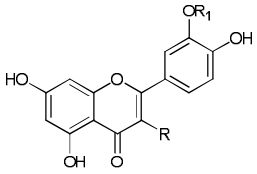

Compound	R	R_1
4	*O*-rha	H
5	*O*-rha-(1→6)-gal	H
6	*O*-rha	CH_3

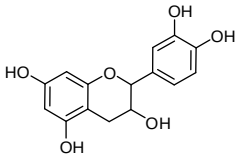

Compound **7**

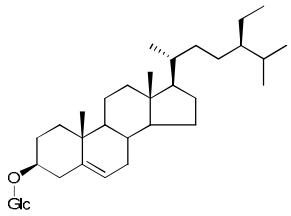

Compound 8

Fig 17: Isolated compounds from *Rumex dentatus* leaves.

hepatocytes, pyknosis of hepatocytic nuclei and focal hepatic hemorrhage (Figs. 2-5) as compared to normal control rats (Fig. 1). CCl_4 treated rats with both leaves and stems of *R. dentatus* as well as silymarin showed slight Kupffer cells activation, few necrosis of sporadic hepatocytes, slight congestion of central vein, few fatty degeneration of hepatocytes and apparent normal parenchyma cells (Figs. 6-8).

On the other hand, kidney of CCl_4-intoxicated rat showed congestion of glomerular tufts, vacuolization of epithelial lining renal tubules, atrophy of glomerular tufts and distension of Bowman's space (Figs. 10-12), as compared to normal control (Fig. 9). However, treatment of intoxicated rats with leaves extract of *R. dentatus* (Fig. 13), showed apparent normal renal parenchyma and no histopathological changes. Treatment of CCl_4-intoxicated rats with total ethanol extract of *R. dentatus* stems (Figs. 14, 15) showed slight congestion of glomerular tufts and slight congestion of intertubular blood capillaries. With respect to, treatment of intoxicated rats with reference silymarin drug, slight dilatation of hepatic sinusoids associated with Kupffer cells activation and no other renal histopathological changes were detected (Fig. 16).

The total phenolic content of leaves and stems was 102 ± 4.01 and 88.68 ± 4.20mg gallic acid equivalents/100 g respectively. Chromatographic separation of aqueous ethanolic extract on Si and Sephadex LH-20 columns afforded eight compounds (Fig. 17). The structures of all known isolates were identified on the basis of interpretation of their chemical, physicochemical analyses (UV, MS, 1D and 2D NMR), comparison with the corresponding published data in the literature and in some cases, comparison with authentic samples for final confirmation. The compounds were identified as: 1,3,8-trihydroxy-6-methyl-9,10-anthraquinone; emodin (**1**), 1,8-dihydroxy-3-methylanthra-9,10-quinone; chrysophanic acid (**2**), 1,5-dihydroxy-3-methyl-9,10-anthraquinone (**3**), quercetin 3-*O*-α-L-rhamnopyranoside (**4**), quercetin 3-*O*-rhamnosyl (1→6)-galactoside (**5**), isorhamnetin 3-rhamnoside (**6**), catchin (**7**), and daucosterol (**8**).

DISCUSSION

Hepatoprotective studies showed that plants have active ingredients that are capable of free radical scavenging in living systems (Nikolova et al., 2011; Kumar et al., 2012). Phenolic compounds are promising bioactive secondary metabolites playing an important role in detoxification of free radicals (Tukan et al., 2006; Shanmugasundaram et al., 2006; Chon et al., 2008). The most important phenolic compounds in *Rumex* plants are flavonoids, anthrones, and anthraquinones (Xu et al., 2004; Zhang et al., 2012). In the present study, a high content of these compounds was detected in the ethanol extract of leaves followed by stems extract suggesting their potential role as antioxidative agents. Evidence suggests that various enzymatic and non enzymatic systems have been developed by the cell to attenuate ROS. However, when a condition of oxidative stress establishes, the defense capacities against ROS becomes insufficient. Therefore, ROS affects the antioxidant defense mechanisms, reduces the intracellular concentration of GSH, decrease the activity of SOD and enhances lipid peroxidation (Khan et al., 2012). In agreement with these explanations, the observed decrease in SOD was recorded in CCl_4 treated rats that might be due to inactivation of the antioxidative enzymes. This may cause an increased accumulation of superoxide radicals, which could further stimulate lipid peroxidation. In addition, the inhibition in GSH concentration can affect redox equilibrium leading to enhanced lipid peroxidation processes. Treatment with either leaves or stems extract of *R. dentatus* normalized the antioxidant levels through their high content of flavonoids and anthraquinones as they have the ability to scavenge free radicals.

Silymarin as an antioxidant flavonoid complex derived from the herb milk thistle (*Silybum marianum*), has the ability to attenuate free radicals elevation, chelates metal ions, inhibits lipid peroxidation and prevents liver glutathione depletion (El-Hawary et al., 2011).

ALT and AST have been reported to be sensitive indicators of liver injury (Motawi et al., 2011). Significant elevation of ALT and AST in CCl_4 group is in agreement with

those reported studies (Lee et al., 2007; Motawi et al., 2011). In addition, CCl_4 induced changes in the process of protein synthesis. Hence, significant decrease in total protein content can be deemed as a useful index of the severity of cellular dysfunction in liver diseases as clearly shown in our studies. Stimulation of protein synthesis has been advanced as a contributory self healing mechanism, which accelerates liver regeneration process. The significant increase in AST, ALT, GGT and ALP as well as total urea and creatinine in CCl_4 group in the present study is in agreement with Reyes-Gordillo et al. (2007) who recorded significant increase in liver enzymes and kidney function post CCl_4 intoxication of rats. The authors added that, the GGT is an indicator of bile duct lesions and its determination alone is considered as a poor indicator of cytotoxicity and the combination of other markers like AST and ALT has been suggested for accurate detection and early diagnosis (Ali et al., 2013). Serum enzymes elevation may be explained by the basis of increase in hepatic cell membrane fluidity and permeability that led to enzyme release into circulation (El-Hawary et al., 2011).

Treatment with leaves or stems extract of *R. dentatus* attenuated the increased level of serum enzymes and caused a subsequent recovery towards normalization. This gives an additional support that *R. dentatus* extracts are able to restore hepatocytes, accelerate regeneration of parenchyma cells, and protects against membrane fragility and decrease leakage of the enzymes into circulation. Therefore, plant extracts acted by the same mode of action of silymarin (El-Hawary et al., 2011). The observed decrease in SDH after CCl_4 intoxication was in parallel with the finding of Rusu et al. (2005). This decrease in enzyme activity was attributed to the increase in free radicals that affected the inner mitochondrial membrane and intracellular calcium stores leading to structural and functional disorganization, overall loss in energy production, irreversible damage, and loss of enzymatic activity. The decrease in hepatic LDH after CCl_4 intoxication was confirmed (Rusu et al., 2005). Enzyme inhibition was mainly due to increase membrane fluidity as a result of ROS involvement leads to enzyme leakage into circulation. The repair mechanisms after treatment may be explained on the basis of enhancement in phospholipids content of cell membrane that coupled with thymidylate synthetase and thymidine kinase enhancing activities confirming liver regeneration (Motawi et al., 2011).

Injury of hepatocytes results in the recruitment and stimulation of inflammatory cells, as well as resident ones, including Kupffer cells. Factors released by these inflammatory cells lead to activation of HSCs and their transformation into a myofibroblast-like phenotype. Chronically activated HSCs produce large amounts of extracellular matrix proteins (ECM) and enhance fibrosis by secreting a broad spectrum of cytokines such as TGF-β_1. This exerts pro-fibrotic actions in other cells and in an autocrine manner perpetuates their own activation (Xu et al., 2004). This is accompanied by a decrease in anti-inflammatory cytokines such as IL-10 and increase in IL-2 and IL-6 (Moron et al., 1979). Oxidative stress, including the decrease of antioxidant capacity, plays an important role in the pathogenesis of liver fibrosis *via* different pathways (Ali et al., 2013). Increased ROS, reactive nitrogen species (RNS), and MDA, are commonly detected in most types of experimental liver fibrosis (Nishikimi et al., 1972). Oxidative stress induces activation of HSCs through the direct effects of ROS, reactive aldehyde products of lipid peroxidation and finally *via* the reaction of NO with ROS, yielding peroxynitrite ($ONO\bar{O}$). The latter is a very reactive, toxic and strongly oxidizing compound, able to induce DNA damage and lipid peroxidation. This process leads to membrane damage and correlates positively with fibrosis through inducing fibrogenic cytokines and increasing collagen synthesis in fibroblasts and hepatic stellate cells (HSCs) (Reyes-Gordillo et al., 2007).

Hepatic fibrosis is usually initiated by hepatocyte damage, leading to the recruitment of inflammatory cells and platelets with the subsequent release of cytokines, chemokines, and growth factors (Khan et al., 2012). These factors probably affect the inflammatory and repairing phase of liver fibrosis by activating HSCs (Khan et al., 2012). This is accompanied by down-regulation of anti-inflammatory cytokines, which has an important role in attenuating the progression of fibrosis (Moron et al., 1979). In parallel with the above information, the present study revealed that, the hepatotoxic agent, CCl_4, leads to pronounced increment in serum pro-inflammatory fibrogenic cytokine, TGF-β_1, IL-2, IL-6 and CRP .These results are confirmed by previous studies indicating the alterations in these cytokines in response to liver fibrosis (Lee et al., 2007).

Regulatory effect of *R. dentatus* extracts on hepatic marker enzymes was documented in our study as free radicals scavengers that could in turn normalize microsomes, lysosomes, mitochondria and plasma membranes permeability and integrity which help to restore the hepatic enzymes to their normal levels. The current study evaluates the *in vivo* role of *R. dentatus* in protecting the liver against injury and fibrogenesis caused by CCl_4 in rats and further explores the underlying mechanisms. We hypothesize that *R. dentatus* might protect the liver from CCl_4 caused injury and fibrogenesis by attenuating oxidative stress and suppressing inflammation. This report demonstrates that *R. dentatus* significantly protects the liver and kidney from injury by reducing the activities of serum AST, ALT, GGT ,total urea and creatinine ,as well as by improving the hepato-renal histological architectures of intoxicated rats. In addition, *R. dentatus* attenuates oxidative stress by increasing content of hepatic GSH, antioxidant enzymes; SOD, catalase and GPX leading to the reduction in the level of both lipid hydroperoxide and *R. dentatus* dramatically suppresses inflammation by regulation of inflammatory cytokines, including TNF-α, IL-2, IL-6 and CRP.

The leaves contained higher percentage of total phenolic than the stems. Phytochemical investigation of leaves resulted in the identification of three anthraquinones, four flavonoids in addition to one glucosyl sterol.

Fractionation of ethanolic bioactive fraction on Si and Sephadex LH-20 columns afforded eight compounds (Fig.17).

Chromatographic properties of compounds **1-3** and the fact that they turned red with sodium hydroxide indicated their

anthraquinonoid nature. The UV spectra revealed the absorption bands characteristic of α-hydroxyanthraquinone. Compound (**1**) EI-MS showed peak at *m/z* 270. ^{1}H NMR spectrum showed two singlets each of one H at δ12.30 and 12.12 pointing to two *peri*-hydroxy protons present in C-8 and C-1, respectively, around the quinone system. The spectrum displayed also two aromatic systems bearing individually two *meta*-coupled protons and one of them bears an aromatic bounded methyl group at δ2.46. The compound was identified as emodin, which was further recognised during a comparison of the data with literature (Abd El-Fattah et al., 1994) as well as authentic sample.

Compound (**2**) EI-MS showed peak at *m/z* 254. The ^{1}H NMR spectra displayed two aromatic systems, one containing an *O*- and *m*-coupled protons of 1,2,3-trisubstituted aromatic system, and two *meta* coupled protons of another aromatic system along with an aromatic bounded methyl signal (δ 2.43). The ^{13}C NMR confirmed the carbonyl of C-9 (δ 189.4) is flanked between two *peri*-hydroxy groups (OH-1,8). Additionally, five methine carbon signals were in the region of δ 136.9 ~ 112.3 and four other quaternary carbon signals between δ145.5 ~ 116.2. In the aliphatic region one methyl carbon signals was at δ 23.5. This confirms the compound as 1,8-dihydroxy-3-methylanthraquinone; chrysophanic acid which was supported by comparison with literature (Abd El-Fattah et al., 1994).

Compound (**3**) EI-MS showed a peak at *m/z* 254 corresponding to $[M]^+$. ^{1}H NMR spectrum of compound **3** exhibited five aromatic signals each of 1H corresponding to one 1,2,3-trisubstituted aromatic ring and two *meta*-coupled protons. In aromatic bounded methyl group was shown as singlet δ 2.48, in contrast to the included singlet of 2H at δ12.97 of *peri*-hydroxy proton in compound **2**, they were shown as two singlets each of 1H at δ 12.13 and 12.02 pointing mostly to two *peri*-hydroxy protons present in two opposite directions (C-1 and C-5) around the quinone system. In ^{13}C NMR of compound **3** displayed similarly 15 carbon signals as in compound **2**; two of them were shown at δ192.4 and 192.3 characteristic for quinone system with two equivalent *peri*-hydroxy groups. Thus the compound **3** was confirmed to be as 1,5-dihydroxy-3-methylanthraquinone which was further confirmed by comparonis the data with literatures (Lu et al., 1992) and it was reported in *R. pulcher* (Harborne and Mokhtari, 1997).

Compound (**4**) UV spectral data can suggest the structure to be 5,7,3',4'-tetrahydroxy flavone 3-*O*-glycoside. Acid hydrolysis showed quercetin and rhammnose (by Co-PC). A molecular ion peak at *m/z* 447 $[M-H]^-$, corresponding to a Mwt of 448, was detected in its (-) ESI-MS spectrum together with two adduct ion peaks with Cl^- and dimolecule at *m/z* 483 and 895, respectively. In the aromatic region of its ^{1}H NMR, the characteristic five ^{1}H resonances of two spin coupling systems for a quercetin 3-*O*-glycoside structure were assigned to H-2', H-6', H-5' (1st system) and H-8 and H-6 (2nd system). Concerning the sugar moiety, signals at δ 5.29 (assignable to an anomeric proton as brs), 3.98 (brs of H-2"), 3.53 (dd, H-3") and 0.88 ppm (for CH_3-6") were characteristic for α–L-rhamnopyranosyl moiety at OH-3. APT ^{13}C NMR spectrum showed resonances of C-4' and C-3' at δ 148.7 and 145.8. Glycosidation at OH-3 was proved by the relative upfield shift of C-3 to 134.9 (Δ~ - 3-4 ppm) and downfield shift of C-2 (Δ~+10 ppm) relative to those of free aglycone. The compound was as quercetin 3-*O*-α-L-rhamnopyranoside (Agrawal and Bansal, 1989).

The physicochemical properties of compounds (**4**)-(**6**) (color under UV light, change with ammonia vapor and responses towards spray reagents, II and III) can suggest their flavonoid glycosides character. On the basis of physicochemical properties and UV spectral data, compounds (**4**) and (**5**) were expected to be quercetin-3-glycoside and compound (**6**) as isorhamnetin aglycone. Acid hydrolysis of the three compounds afforded quercetin as an aglycone and L-rhamnose for compound (**4**) and (**6**), L-rhamnose and D-galactose for (**5**) (Markham, 1982; Harborne and Mabry, 1982).

The presence of sugar moiety for compound (**5**) was evidenced from the two resonances at 4.60 ppm (*J*= 7.5 Hz) and 4.24 ppm broad singlet assigned to the two anomeric proton signals of β-galactosyl and α-rhamnosyl moieties, respectively. Anomeric carbons of the sugar moieties appeared at 99.4 and 100.8 ppm indicating *O*-linked sugar. The downfield shift of C-6" (66.9 ppm) of galactose which appeared ~ 6.0 ppm downfield showed 6"→1'" linkage of D-galactose and L-rhamnose which established the structure as quercetin-3-*O*-α-L-rhamnopyranose-1'"→6"-β-D-galactopyranoside (Agrawal and Bansal, 1989).

UV spectrum of compound (**6**) showed the presence of free 7-hydroxyl group in ring A which is manifested by an intensive bathochromic shift or band II in addition of NaOAc as shift reagent. The bathochromic shift of band I on NaOMe spectrum confirmed the presence of a free OH at C-4'. Complete acid hydrolysis afforded isorhamnetin and rhamnose (by Co-PC). ^{1}H NMR spectrum showed the downfield shift of H-2' to δ 7.32 indicated that the methoxyl group is located at position 3' to confirm the identity of the aglycone as isorhamnetin. Also, singlet proton of the methoxy group at δ 3.99 was found. The signal of the anomeric proton of the rhamnose moiety appeared as a doublet at δ 5.21 (*J*=1.2 Hz) and methyl rhamnosyl protons at δ 0.90 as a doublet (*J*=6 Hz). The configuration was confirmed by the coupling constant 1.2 Hz as α-L-rhamnose. The compound (**6**) was identified as isorhamnetin 3- *O*-α-L-rhamnoside. In ^{13}C NMR spectrum it was observed that the C-3 is shifted downfield at δ 134.1 ppm indicating that the linkage between the sugar unit and the aglycone is at C-3. Also, it was observed that the C-3' is shifted downfield at δ 147.2 ppm indicating that C-3' is substituted. The spectrum showed methoxy group at δ 56.0 ppm and one anomeric carbon at δ 101.8 ppm and a methoxy group at δ 17.4 ppm corresponding to -α-L-rhamnose (Iwashina and Ootani, 1990).

UV spectra of compound (**7**) can suggest the presence of the isolated benzenoid chromophores.In the aromatic region of its ^{1}H NMR, the characteristic five hydrogen resonances of the

positions 6, 8, 2', 5' and 6' of a flavonoid skeleton were observed. A doublet (*J*=2.4 Hz) at δ 5.89 assigned to H-8 showed *meta*–coupling with doublet (*J*=2.1 Hz) at δ 5.70 assigned to H-6. On the other hand, the doublet (*J*=2.1 Hz) at δ 6.74 assigned to H-2' showed *meta*–coupling with doublet of doublet (*J*=1.8, 6.5 Hz) at δ 6.60 assigned to H-6' and the later exhibited an *ortho*-coupling with doublet (*J*=8.1 Hz) at δ 6.69 assigned to H-5'. The spectrum indicated that compound (**7**) is a catechin-type flavanol with *trans*-configuration at C-2 and C-3 (coupling constant between H-2 and H-3 was 7 Hz). The compound was identified as catechin (Nonaka et al., 1983).

Compound (**8**) m.p. and gave positive Liebermann-Burchard for sterol. The mass spectrum and NMR spectroscopic measurements 1D ^{1}H- and APT and 2D ^{1}H-^{1}H COSY, HMQC and HMBC and by the aid of the published data the compound was identified as 3-*O*-glucopyranosyl-β-sitosterol (daucosterol) (Anton et al., 1993; Faizi et al., 2001). Inspection of the APT spectrum of showed the existence of 35 signals, the sugar moiety gives rise to one methylene group and five methine groups, whereas the aglycone part exhibits twenty-nine carbon signals, arising from six methyl groups, eleven methylene groups, nine methine groups and three quaternary carbon atoms. The aglycone moiety was identified as β-sitosterol from its ^{1}H and APT spectra. The sugar moiety was connected to C-3 atom as shown from its HMBC spectrum cross peaks H-1`/C-3. The sugar moiety was identified as glucopyranose from its ^{1}H-NMR, APT, ^{1}H-^{1}H COSY and HMQC spectra. Acid hydrolysis confirmed the presence of glucose in aqueous layer and the organic layer contained β-sitosterol as compared with authentic reference sample. The data were compared with the literature and the compound was identified as β-sitosterol-3-*O*-glucopyranoside, which was previously isolated from *R. dentatus* roots growing in China (Zhu et al., 2006).

Quinones constitute a structurally diverse class of phenolic compounds with a wide range of pharmacologial properties, which are the basis for different applications in the broad field of pharmacy and medicine. In traditional medicine all over the world, genus of *Rumex* which is rich in quinones is used for the treatment of a variety of diseases (Xu et al., 2004; El-Hawary et al., 2011). Some anthraquinones were reported to have hepatoprotective and antiproliferative effect (Kumar et al., 2007; Zargar et al., 2011).

In the current study, one of the bioactive secondary metabolites is the anthraquinones (Fig. 17). The most abundant compound of *R. dentatus*, emodin was previously reported to possess immunostimulant, anti-inflammatory activity, and protective effects on hepatocytes and cholangiocytes against α-naphthyl *iso*thiocyanate-induced cholestatic liver injury in rats (Zhao et al., 2009).

In the present study, chrysophanic acid was isolated as another anthraquinone from *R. dentatus*. It was reported to display anti-inflammatory (Kim et al., 2010), and hepatoprotective (Zhao et al., 2009) activities. The anti-inflammatory capability was reported to act through suppression of the activation of nuclear factor-κB (NF-κB) and caspase-1. Also, the identified bioactive compound; 1,8-dihydroxy-3-hydroxymethyl anthraquinone was reported as hepatoprotective agent (Kim et al., 2010). In another study, the emodin derivative (emodin-3-methyl ether), physcion showed hepatoprotective (Zhao et al., 2009) and anti-inflammatory (Kim et al., 2010) activity.

Three flavonoid glycosides were isolated from *R. dentatus* in the present study. Compounds (**4**) and (**5**) were identified as quercetin derivatives. Flavonoids were reported as classes of bioactive constituents showing hepatoprotective activity (Kumar et al., 2012; Shalaby et al., 2012). Certain quercetin glycoside isolated from *R. aquaticus* Herba was reported as a protective agent against ethanol-induced cell damage. The cytoprotective effect of this flavonoid may involve inhibition of ROS generation and downstream activation of the *ERK* 1/2 in feline esophageal epithelial cells (Cho et al., 2011). Another study reported that quercetin glycoside, hyperoside (quercetin-3-galctoside) has protective effect against CCl_4-induced liver damage in mice and this protection is likely due to enhancement of the antioxidative defense system and suppression of the inflammatory response (Choi et al., 2011). Rutin was previously isolated from *R. dentatus*. The hepatoprotective effect of rutin against CCl_4-induced oxidative stress and its role in alleviation of lipid peroxidation and restoration of p53 and CYP2E1 activity were reported (Khan et al., 2012). In the current study, daucosterol was isolated from *R. dentatus* leaves. This steroidal glycoside was previously isolated together with different steroids as main constituents from the hepatoprotective plant; *Imperata cylindrical* (Mohamed et al., 2009). β-Sitosterol, β-sitosterol glucoside, chryasophanic acid, quercetin, aloe emodin glucoside, rutin have been isolated from *Ficus ingens* as the main bioactive compounds. The hepatoprotective effect of this plant was suggested to be attributed to its phytochemical constituents (mainly polyphenolic compounds) with their antioxidant and membrane stabilizing properties (Donia et al., 2013). Also, catechin was also identified in the current study. Hepatoprotective potential of *R. vesicarius* extract against hepatotoxicity induced by CCl_4 was reported (El-Hawary et al., 2011). In which, catechin was investigated as one of bioactive compounds in plant extract. Hepatoprotective effect of semen of *R. crispus* (Lee et al., 2007) was reported. Protective effect of *R. patientia* (English Spinach) roots on ferric nitrilotriacetate (Fe-NTA) induced hepatic oxidative stress was explored (Lone et al., 2007). Its liver protection activity was expected to be due to the presence of anthraquinones and other phenolic compounds.

Antioxidant capacity of *R. dentatus* was reported (Elzaawely et al., 2012) and it may be attributed to its polyphenolic compounds as flavonoids, anthraquinones, anthrones, naphthalenes glycosides (Zhang et al., 2012).

This study demonstrates that *Rumex* protects the rat liver from CCl_4-caused injury and fibrogenesis by suppressing hepatic inflammation and attenuating hepatic oxidative stress. Our results

suggest that *R. dentatus* might be a therapeutic antifibrotic agent for the treatment of hepatic fibrosis.

CONCLUSION

Rumex dentatus L has the ability to down regulate free radicals elevation, improve liver and cholestatic biomarkers, ameliorate hepatic marker enzymes, reduce fibrosis severity and normalize the hepatic cells architecture. The ethanol extract of leaves recorded potent effect in improving the selected parameters. The hepatoprotective effect of *R. dentatus* L demonstrated in this study may explore its nutraceutical role in human diet. The isolated bioactive phytochemicals was suggested to be responsible for the pronounced pharmacological activity. Therefore, further studies are needed for its clinical application.

REFERENCES

Abd El-Fattah H, El-Dahmy GS, Hubaishi A. Phytochemical investigation of *Rumex luminiastrum*. Acta Pharm Hungarica, 1994; 64: 83-85.

Agrawal PK, Bansal MC. ^{13}C NMR of Flavonoids. In: Studies in organic chemistry 39, Agrawal P K (editor). New York, Elsevier Science 1989; 283-364.

Ali SA, Hamed MA, El- Rigal NS, Shabana MH, Kassem MES. Chemical constituents of *Argyreia speciosa* Fam. Convolvulaceae and its role against hyperglycemia. J Appl Pharm Sci 2011; 1:76-84.

Anton R, Jiang Y, Weniger B, Beck JP, Rivier L. Pharmacognosy of *Mimosatenuiflora* (Willd.) Poiret. J Ethnopharmacol 1993; 38:153-157.

Babson AL, Babson SR. Kinetic colorimetric measurement of serum lactate dehydrogenase activity. Clin Chem, 1973; 19: 766-769.

Bloch A, Thomson CA. Position of the American Diabetic Association: phytochemicals and functional foods. J Am Diet Assoc 1995; 95: 406-493.

Boulos L, El-Hadidi MN. 1984. The Weed Flora of Egypt. The American University *in* Cairo Press, Cairo, pp178.

Bradford MM. A rapid and sensitive method for the quantitation of microgram quantities of protein utilizing the principle of protein-dye binding. Anal 1976; 72: 248-254.

Buege JA, Aust SD: Microsomal lipid peroxidation. Meth Enzymol 1978; 52: 302-310.

Cakmak I, Marschner H. Magnesium deficiency and high light intensity enhance activities of Superoxide dismutase, ascorbate peroxidase, and glutathione reductase in bean leaves. Plant Physiol 1992; 98: 1222-1227.

Cho JH, Park SY, Lee HS, Whang WK, and Sohn UD. The Protective Effect of quercetin-3-*O*-β-D-glucuronopyranoside on ethanol-induced damage in cultured feline esophageal epithelial cells. Korean J Physiol Pharmacol 2011; 15: 319–326.

Choi JH, Kim DW, Yun N, Choi JS, Islam MN, Kim YS, Lee SM. Protective effects of hyperoside against carbon tetrachloride-induced liver damage in mice. J Nat Prod 2011; 74: 1055-1060.

Chon SU, Heo BG, Park YS, Cho JY, Gorinstein S. Characteristics of the leaf parts of some traditional Korean salad plants used for food. J Sci Food Agric 2008; 88: 1963-1968.

Donia AM, Soliman GA, Zaghloul AM, Alqasoumi SI, Awaad AS, Radwan AM, Basodan OA. Chemical constituents and protective effect of *Ficus ingens* (Miq.) Miq. on carbon tetrachloride-induced acute liver damage in male Wistar albino rats. J Saudi Chem Soc 2013; 17: 125-133.

El-Hawary SA, Sokkar NM, Ali ZY, Yehia MM. A profile of bioactive compounds of *Rumex vesicarius* L. J Food Sci 2011; 76: C1195-C1202.

Elzaawely AA, Tawata S. Antioxidant capacity and phenolic content of *Rumex dentatus* L. grown in Egypt. J Crop Sci Biotechnol 2012; 15: 59-64.

Faizi MA, Saleem R, Irfanullah SB. Complete 1H and 13C NMR assignments of stigma-5-en-3-*O*-b-glucoside and its acetyl derivative. Magn Reson Chem 2001; 39: 399-405.

Gella FJ, Olivella T, Cruz PM, Arenas J, Moreno R, Durban R, et al. A simple procedure for routine determination of aspartate aminotransferase and alanine aminotransferase with pyridoxalphosphate. Clin Chem Acta 1985; 153: 241-247.

Harborne JB, Mabry TJ. 1982. The Flavonoids: Advances in researches, Chapter 2: Chapman and Hall Ltd, London.

Harborne JB, Mokhtari N. Two sulphated anthraquinone derivatives in *Rumex pulcher*. Phytochem 1997; 16: 1314-1315.

Iwashina T, Ootani S. Three flavonol allosides from *Glaucidium palmatum* Phytochemistry 1990; 29: 3639-3641.

Khan RA, Khan MR, Sahreen S. CCl_4-induced hepatotoxicity: protective effect of rutin on p53, CYP2E1 and the antioxidative status in rat. BMC Complement Altern Med 2012; 8: 172-178.

Kim SJ, Kim MC, Lee BJ, Park DH, Hong SH. Um JY Anti-inflammatory activity of chrysophanol through the suppression of NF-κB/caspase-1 activation *in vitro* and *in vivo*. Molecules 2010; 15: 6436-6451.

Kumar SV, Sanjeev T, Ajay SA. Review on hepatoprotective activity of medicinal plant. IJARPB 2012; 1: 31-38.

Lee SS, Kim, DH, Lee S. Anti-Inflammatory, analgesic and hepatoprotective effect of Semen of *Rumex crispus*. Korean J Pharmacogn 2007; 38: 334-338.

Lone IA, Kaur G, Athar M, Alam M S. Protective effect of *Rumex patientia* (English Spinach) roots on ferric nitrilotriacetate (Fe-NTA) induced hepatic oxidative stress and tumor promotion response. Food Chem Toxicol 2007; 45: 1821-1829.

Lu XZ, Xu WH, Naoki H. Anthraquinones from *Salvia przewalskii*. Phytochemistry 1992; 31: 708-709.

Lundh, HAB. Sequence comparison between kidney and liver lesions in the rat following carbon tetrachloride poisoning. J Occup Med 1964; 6: 123-128.

Markham KR. 1982. Techniques of flavonoid identification, Academic press, London.

Marsillach J, Camps J, Ferré N, Beltran R, Rul A, Mackness B, et al. Paraoxonase-1 is related to inflammation, fibrosis and PPAR delta in experimental liver disease. BMC Gastroenterol 2009; 9: 3.

Mohamed GA, Abdel-Lateff A, Fouad MA, Ibrahim SR M, Elkhayat ES, Okino T. Chemical composition and hepato-protective activity of *Imperata cylindrical* Beauv. Pharmacogn Mag 2009; 5: 28-36.

Mohandas J, Marshal JJ, Duggin GG, Horvath JS, Tiller DJ. Differential distribution of glutathione and glutathione-related enzymes in rabbit kidney. Possible implications in analgesic nephropathy. Biochem Pharmacol 1984; 33: 1801–1807.

Moron MS, Depierre JW, Mannervik B. Level of glutathione, glutathione reductase and glutathone-S-transferase activities in rat lung and liver. Biochim Biophys Acta 1979; 582:67-78.

Motawi TK, Hamed MA, Shabana MH, Hashem RM, Aboul-Naser AF *Zingiber officinale* acts as a nutraceutical agent against liver fibrosis. Nutr Metab 2011; 8: 40-51.

Nikolova M, Evstatieva L, Nguyen TD. Screening of plant extracts for antioxidant properties. Botanica Serbica 2011; 35: 43-48.

Nishikimi M, Rae NA, Yagi K. The occurrence of superoxide anion in the action of reduced phenazine methosulphate and molecular oxygen. Biochem Biophys Res Commun 1972; 46: 849-853.

Nonaka G, Ezaki E, Hayashi K, Nishiioka J. Flavonol glucosides from rhubarb and *Rhaphiolepis umbellate*. Phytochemistry, 1983; 22: 1659-1661.

Raghavendra M, Reddy AG. Acute and chronic toxicity studies of ethanolic extract of *Rumex vesicarius* L in experimental animals. J Sci 2011; 1: 16-20.

Recknagel RO, Glende Jr EA, Dolak JA, Waller RL. Mechanisms of carbon tetrachloride toxicity. Pharmacol Ther 1989; 43:139–154.

Reyes-Gordillo K, Segovia J, Shibayama M, Vergara P, Moreno MG, Muriel P. Curcumin protects against acute liver damage in the rat by

inhibiting NF-kappa B, pro inflammatory cytokines production and oxidative stress. Biochem Biophys Acta 2007; 1770: 989-996.

Rice ME, Shelton E. Comparison of the reduction of two tetrazolium salts with succinoxidase activity of tissue homogenates. J Nat Cancer Inst 1957; 18: 117-125.

Rosalki SB, Foo AY, Burlina A. Multicenter evaluation of *iso*-ALP test kit for measurement of bone alkaline phosphatase activity in serum and plasma. Clin Chem 1993; 39: 648-652.

Rusu MA, Tamas M, Puica C, Roman I, Sabadas M. The hepatoprotective action of ten herbal extracts in CCl_4 intoxicated liver. Phytother Res 2005; 19: 744-749.

Shalaby NMM, Abd-Alla HI, Hamed MA, Al-Ghamdi SN, Jambi SMS. Flavones composition and therapeutic potential of *Dodonaea viscosa* against liver fibrosis. Int J Phytomed 2012; 4: 27-39.

Shanmugasundaram P, Venkataraman S. Hepatoprotective and antioxidant effects of *Hygrophila auriculata* (K. Schum) Heine Acanthaceae root extract. J Ethnopharmacol 2006; 104: 124-128.

Singleton VL, Rossi JA. Colorimetry of total phenolics with phosphomolybdic phosphotungstic acid reagents. Am J Enol Vitic 1965; 16:144-158.

Sreejayan N, Rao MNA. Nitric oxide scavenging by curcuminoids. J Pharm Pharmacol 1997; 49: 105-107.

Suzuki H, Suzuki K: Rat hypoplastic kidney (*hpk/hpk*) induces renal anemia, hyperparathyroidism, and osteodystrophy at the end stage of renal failure. J Vet Med Sci 1998; 60: 1051-1058.

Szasz GA. kinetic photometric method for serum γ-glutamyltranspeptidase. Clin Chem 1969; 15: 124-136.

Tukan SK, Takruri HR, Al-Eisawi DM. The use of wild edible plants in the Jordanian diet. Int J Food Sci Nutr 1998; 49: 225-235.

Xu JY, Su YY, Cheng JS, Li SX, Liu R, Li WX, et al. Protective effects of fullerenol on carbon tetrachloride-induced acute hepatotoxicity and nephrotoxicity in rats. Carbon 2010; 1388-1396.

Xu MS, Wang ZY, Kang YH. Recent advance on the chemistry and bioactivity of genus *Rumex*. Chin Arch Tradi Chin Med 2004; 22: 417-420.

Yuvaraj P, Subramoniam A. Hepatoprotective property of *Thespesia populnea* against carbon tetrachloride induced liver damage in rats. J Basic Clin Physiol Pharmacol 2009; 20:169-177.

Zargar BA, Masoodi MH, Ganie AB, Showkat A. Phytoconstituents and therapeutic uses of *Rheum emodi* wall. ex Meissn. Food Chem 2011; 128: 585-589.

Zhang H, Guo Z, Wu N, Xu W, Han L, Li N, et al. Two novel naphthalene glucosides and an anthraquinone isolated from *Rumex dentatus* and their antiproliferation activities in four cell lines. Molecules 2012; 17: 843-850.

Zhao YL, Wang JB, Zhou GD, Shan LM, Xiao XH. Investigations of free anthraquinones from rhubarb against α-naphthylisothiocyanate-induced cholestatic liver injury in rats. Basic Clin Pharmcol Toxicol 2009; 104: 463-469.

Zhu JJ, Zhang CF, Zhang M, Wang ZT. Studies on chemical constituents in roots of *Rumex dentatus*. Zhongguo Zhong Yao Za Zhi. 2006; 31: 1691-1693.

How to cite this article:

Naima Z. Mohamed, Howaida I. Abd-Alla, Hanan F. Aly, Mona Mantawy, Nehal Ibrahim, Sohair A. Hassan. CCl_4-induced hepatonephrotoxicity: protective effect of nutraceuticals on inflammatory factors and antioxidative status in rat. J App Pharm Sci, 2014; 4 (02): 087-100.